A Novel Method for Imaging Apoptosis Using a Caspase-1 Near-Infrared Fluorescent Probe[1]

Shanta M. Messerli, Shilpa Prabhakar*, Yi Tang†, Khalid Shah*,†, Maria L. Cortes*, Vidya Murthy*, Ralph Weissleder†, Xandra O. Breakefield*,† and Ching-Hsuan Tung†*

*Departments of Neurology and Radiology, Massachusetts General Hospital and Neuroscience Program, Harvard Medical School, Boston, MA 02115, USA; †Center for Molecular Imaging Research, Massachusetts General Hospital, Harvard Medical School, Charlestown, MA 02129, USA

Abstract

Here we describe a novel method for imaging apoptosis in cells using a near-infrared fluorescent (NIRF) probe selective for caspase-1 (interleukin 1β–converting enzyme, ICE). This biocompatible, optically quenched ICE-NIRF probe incorporates a peptide substrate, which can be selectively cleaved by caspase-1, resulting in the release of fluorescence signal. The specificity of this probe for caspase-1 is supported by various lines of evidence: 1) activation by purified caspase-1, but not another caspase *in vitro*; 2) activation of the probe by infection of cells with a herpes simplex virus amplicon vector (HGC-ICE-lacZ) expressing a catalytically active caspase-1–lacZ fusion protein; 3) inhibition of HGC-ICE-lacZ vector–induced activation of the probe by coincubation with the caspase-1 inhibitor YVAD-cmk, but not with a caspase-3 inhibitor; and 4) activation of the probe following standard methods of inducing apoptosis with staurosporine, ganciclovir, or ionizing radiation in culture. These results indicate that this novel ICE-NIRF probe can be used in monitoring endogenous and vector-expressed caspase-1 activity in cells. Furthermore, tumor implant experiments indicate that this ICE-NIRF probe can be used to detect caspase-1 activity in living animals. This novel ICE-NIRF probe should prove useful in monitoring endogenous and vector-expressed caspase-1 activity, and potentially apoptosis in cell culture and *in vivo*.

Neoplasia (2004) **6**, 95–105

Keywords: Caspase-1, near-infrared fluorescence (NIRF), apoptosis, brain tumors, HSV.

Introduction

The balance and coordination between cell proliferation and programmed death (apoptosis) is essential for normal physiology. Apoptosis is involved in embryonic development, immune cell processes, and tissue homeostasis. In addition, neurodegenerative disorders, acquired immunodeficiency syndrome, cancer, myelodysplastic syndromes, ischemia/reperfusion injury, and autoimmune disorders all involve inappropriate apoptosis [1]. The transformation of a normal cell to an apoptotic cell is typically characterized by loss of cell volume, plasma membrane blebbing, nuclear chromatin condensation and aggregation, and endonucleocytic degradation of DNA into nucleosomal fragments [2]. These cell changes occur following sequential activation of initiator and effector caspases [3–6]. Once activated, caspases, of which there are at least 14 different mammalian members [7–9], cleave a variety of structural, regulatory, and DNA repair proteins and, by doing so, disrupt important cellular processes and trigger cellular and morphological events associated with cell death [10]. Consequently, caspases are considered both initiators and executioners of apoptosis.

The role that caspases play in immune response and apoptosis is still being elucidated. Caspase-1, also known as interleukin 1β–converting enzyme (ICE), was originally characterized as cleaving inactive prointerleukin 1β to generate the active proinflammatory cytokine interleukin 1β and is considered an initiator caspase [11]. Studies suggest that the activation of caspase-1 is under the control of caspase-11 [12] and that caspase-11, in turn, is involved in caspase-3 activation and apoptosis induced by brain ischemia [13,14]. Caspase-1 is required for apoptosis in Rat-1 fibroblasts as well as other mammalian and insect cells [11,15–17]. Caspase-1 activation is also required for human prostate cancer cells to undergo apoptosis in response to transforming growth factor-β [18], and the majority of primary prostate cancer specimens (80%) have downregulation of caspase-1 expression, implicating this loss as a potential step in malignant progression [19]. Furthermore, studies have demonstrated the activation of caspase-1 in dying motor neurons in a mouse model of Cu^{2+},Zn^{2+} superoxide dismutase–mediated familial amyotrophic lateral sclerosis [20].

Visualization of cellular apoptosis has traditionally used several approaches, including labeling with annexin V [21]

Address all correspondence to: Dr. Xandra O. Breakefield, PhD, Departments of Neurology and Radiology, Molecular Neurogenetics Unit, Building 149, 13th Street, Massachusetts General Hospital, East Charlestown, MA 02129, USA. E-mail: breakefield@hms.harvard.edu

[1]This work was funded by the MGH Medical Discovery award (S.M.M.), the Department of the Army DAMD17-00-1-0537, the Texas Neurofibromatosis Foundation through the Terrill family (X.O.B.), NIH P50-CA86355, R24-CA92782 (R.W.), and R33-CA88365 (C.H.T.).
Received 10 July 2003; Revised 25 November 2003; Accepted 4 December 2003.

and terminal transferase-mediated dUTP nick end labeling (TUNEL) staining [22–24]. For both annexin V and TUNEL staining, cells or tissues must be removed from the animal and fixed, which may inadvertently cause cellular disruption. Examination of the specificity and sensitivity of TUNEL staining reveals a serious drawback in its inability to discriminate apoptotic from necrotic cells because necrotic cells also have free DNA ends after oxidative and toxic injury [25,26].

Technology to monitor apoptosis and activity of specific caspases in living cells is currently under development. Studies have shown that apoptosis can be noninvasively imaged in living cells in real time using a recombinant luciferase reporter molecule that has attenuated levels of activity when expressed in mammalian cells [27]. This reporter molecule is cleaved by caspase-3 in apoptotic cells, resulting in restoration of luciferase activity, which can be detected in living animals with bioluminescence imaging. In a complementary approach, we have investigated a method to image apoptosis noninvasively and dynamically over time using a near-infrared fluorescent (NIRF) probe activated by caspase-1. In previous studies, we have developed a series of novel activatable NIRF probes specific for various proteolytic enzymes, such as cathepsins [28,29], matrix metalloproteinases [30–33], and viral proteases [34]. This novel optical imaging technology has been used for detection of specific protease activities *in vitro*, in culture, and *in vivo* [35]. Here we examined the specificity of a newly developed ICE-NIRF imaging probe with purified enzymes and inhibitors *in vitro*. This probe was also used to monitor caspase-1 expression in association with apoptosis resulting from drugs, irradiation, or infection of cells with a herpes simplex virus (HSV) amplicon vector expressing caspase-1–lacZ in culture and from vector-infected tumor cells *in vivo*.

Materials and Methods

Generation of HSV Amplicons

The caspase-1–lacZ cassette (4.2 kb) was obtained from Dr. Jungying Yuan (Harvard Medical School, Boston, MA) [15] and cloned into the multiple cloning site (MCS) of the HSV amplicon plasmid, pHGCX [36], which contains an HSV origin of replication (ori_s), a cleavage/packaging signal (pac), and an expression cassette for enhanced green fluorescent protein (EGFP; Clontech, Palo Alto, CA) under an intermediate early viral promoter, IE4/5 (Figure 2*A*). The resulting amplicon, termed HGC-ICE-lacZ, was transformed into DH10B-competent cells and DNA from colonies was assessed by restriction digestions. The control amplicons were pHGCX and a version of pHGCX bearing coding sequences for firefly luciferase in the MCS, termed pHGC-Fluc [34].

Cell Culture

The C6BVIK cell line expressing HSV-1 thymidine kinase (TK) was derived from the rat glioma line C6 [37] by Ezzeddine et al. [38]. The human glioma cell line Gli36 was originally obtained from Dr. Anthony Capagnoni (UCLA School of Medicine, Los Angeles, CA). 2-2 cells, Vero-derived cells that constitutively express the HSV-1 ICP27 protein, were kindly provided by Dr. Rozanne Sandri-Goldin (UC Irvine, Irvine, CA) [39]. All cell lines were cultivated in Dulbecco's modified Eagle's medium (DMEM; GIBCO, Carlsbad, CA) containing 100 U/ml penicillin, 100 μg/ml streptomycin (P/S), and 10% fetal bovine serum (FBS; D10P/S) with 500 μg/ml G418 (Geneticin; GIBCO, Carlsbad, CA).

Packaging of Amplicon DNA Into HSV-1 Virions and Titration of Vector Stocks

Vero 2-2 cells were cotransfected with pHGC-ICE-lacZ or pHGC-Fluc, fHSVΔpacΔ27 0+, and pEBH-ICP27 DNA using LipofectAMINE (GIBCO), as described [36]. After 3 days, the cells were scraped into the medium, the suspension was frozen and thawed three times, and cell debris was removed by centrifugation (10 minutes, 1400 × *g*). To concentrate the vector stocks, the supernatant was centrifuged for 2.5 hours at 100,000 × *g* through a 25% sucrose solution in phosphate-buffered saline (PBS), pH 7.4. The pellet was suspended in DMEM containing P/S, 10% FBS, and G418. To determine vector titers [transducing units (tu) per milliliter], 293 cells were infected and, 24 hours later, green fluorescent cells were counted under 488-nm excitation on a Zeiss microscope (Thornwood, NY).

Synthesis of Probe

The NIRF probe was prepared following a previously published protocol [28]. Briefly, a caspase-1–cleavable peptide substrate [Gly-Trp-Glu-His-Asp-Gly-Lys fluorescein isothiocyanate (FITC)-Cys-NH_2] [40] that contains an N-terminal NIR fluorochrome, Cy5.5 (absorption maximum 675 nm, emission maximum 694 nm; Amersham-Pharmacia, Piscataway, NJ), was attached to a biocompatible, partially pegylated poly-L-lysine delivery vehicle through the C-terminal cysteine residue to generate the ICE-NIRF probe (Figure 1*A*). On average, each delivery molecule contained 18 reporter probes with efficient autoquenching of fluorescence.

In Vitro Activation with Purified Caspases

Specific activation of the ICE-NIRF probe was tested in the presence of purified caspase-1 or caspase-3 in PBS buffer. The probe (0.2 μM, 500 μl) was incubated with or without specific caspase (0.25 μg; Calbiochem, San Diego, CA) at room temperature for 30 minutes. NIRF signal was measured using a fluorescence spectrophotometer (U4500; Hitachi, Chula Vista, CA). The excitation and emission wavelengths were set at 675 and 694 nm, respectively. In an inhibition experiment, a caspase-1 specific inhibitor, Ac-Tyr-Val-Ala-Asp-CHO (4 μM; Calbiochem), was added to the caspase-1 ICE-NIRF probe mixture and studied under the same conditions.

Assessment of Apoptosis by NIRF Probe and Annexin, Propidium Iodide (PI), and TUNEL Staining

First, cells were treated with 1 μM ICE-NIRF probe diluted in OptiMEM and incubated for 30 minutes in a 5% CO_2 incubator. Then cells were rinsed twice with PBS

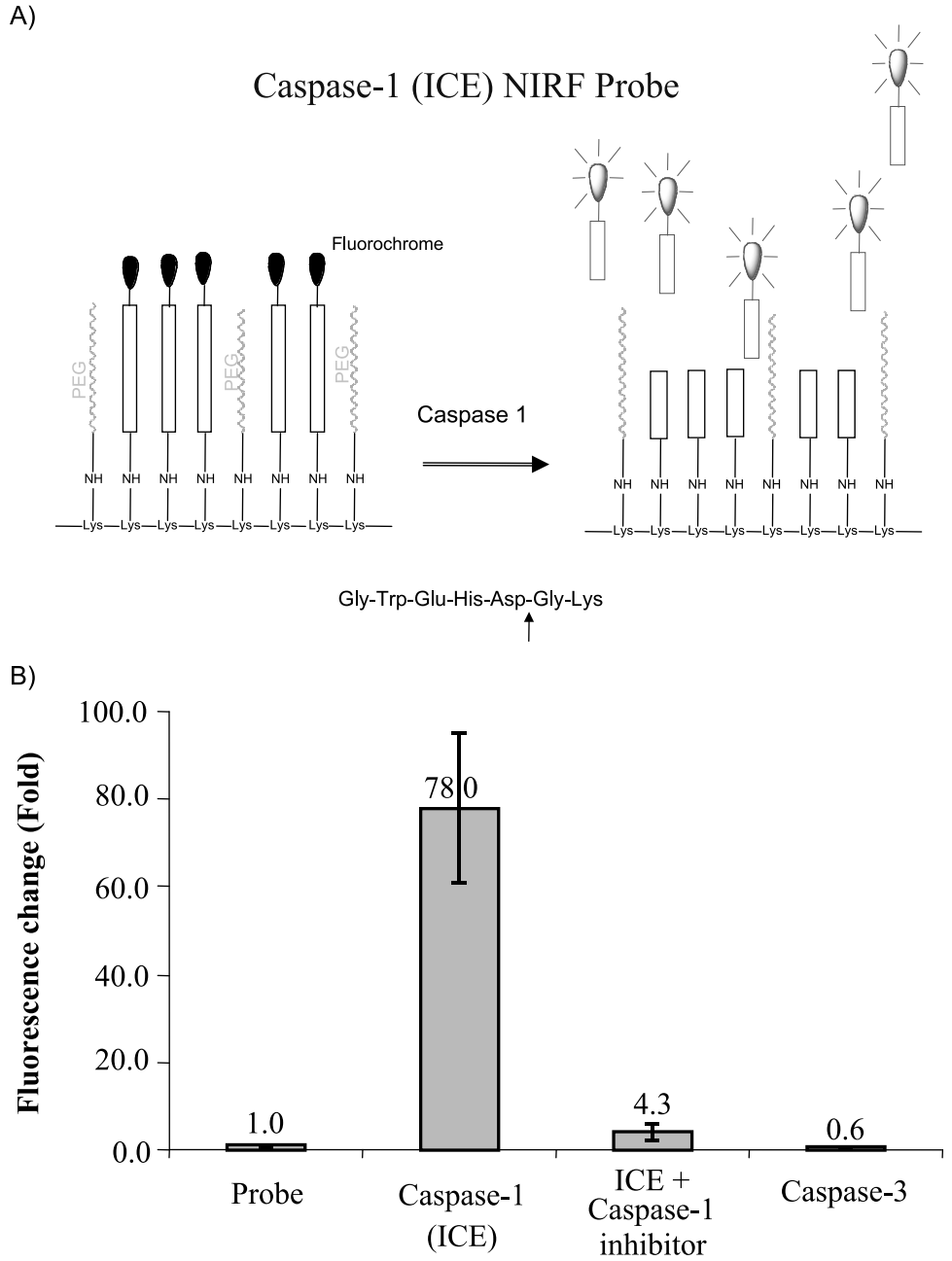

Figure 1. *Characteristics of ICE-NIRF probe. (A) Schematic diagram of the ICE-NIRF probe. In its intact state (left), the high local density of fluorochromes causes substantial fluorescence quenching. The enzymatic activation by caspase-1, involving cleavage of the peptide substrate, results in release of the near-infrared fluorochrome, Cy5.5 (right). (B) Specificity of ICE-NIRF probe using purified caspases. In vitro testing of this caspase-1 NIRF probe indicates that activation is specific to caspase-1. Incubation with purified caspase-1 activated the probe 78-fold, whereas incubation of caspase-3 did not activate the probe. Furthermore, activation of the probe by caspase-1 was blocked by coincubation with a caspase-1 inhibitor.*

and resuspended in 1 × binding buffer (Apoptosis Kit; Clontech) with 0.5 μg/ml annexin V–FITC and, in some cases, 1.25 μg/ml PI per well using the annexin V–FITC Apoptosis Kit (Clontech) and incubated for 5 to 15 minutes in the dark. Following rinsing with OptiMEM, cells were fixed with 2% paraformaldehyde (PFA) for 15 minutes, washed with PBS twice, and mounted using Fluoromount G media (Southern Biotechnology, Birmingham, AL). The slides were observed under the confocal microscope (Zeiss Axiovert 200) using the 633-nm laser to detect the NIRF probe, the 488-nm laser to detect EGFP and annexin, and the 543-nm laser to detect PI staining. Assessment of apoptosis was also performed using TUNEL staining [41] and detected with the 543-nm laser. The LSM 5 Pascal Software (v. 2.8 WS) was used for quantitative analysis of images. The "Profile" function of this software package was used to compute the intensity as a function of distance along a line drawn directly through each image. The intensities were averaged, and the average with the 63-nm laser was normalized to the average with the 488-nm laser.

Drug Treatment

In order to evaluate the specificity of the ICE-NIRF probe, we examined the effects of the caspase-1 inhibitor, YVAD-cmk (Clontech), and the caspase-3 inhibitor, DEVD-fmk (Clontech), on HGC-ICE-lacZ vector–induced probe activation. For these experiments, Gli36 cells were plated at a density of 3×10^5 cells/well in 24-well plates (Becton Dickinson, Franklin Lakes, NJ), and infected 24 hours later with either HGC-ICE-lacZ or HGC-Fluc vector. Vectors were used at a multiplicity of infection (MOI) = 1 tu/cell, at which over 90% of cells were infected as assessed by EGFP fluorescence. For the caspase-1 inhibitor, 24 hours after being plated, cells were coincubated with 25 μM YVAD-cmk and HGC-ICE-lacZ vector (MOI = 1) for 24 hours. For the caspase-3 inhibitor, a parallel experiment was carried out using 10 μM DEVD-fmk. To evaluate caspase-1 activity and apoptosis, cells were assessed for NIRF probe activation and annexin and TUNEL staining, as above. Tetrazolium salt WST-1 cell viability assays were performed to confirm that these inhibitors were not toxic to Gli36 cells under these conditions.

To induce apoptosis, Gli36 cells were exposed to 50 μM staurosporine (Sigma, St. Louis, MO) for 24 hours, then washed twice in PBS and evaluated for ICE-NIRF probe fluorescence and annexin staining. Control cells were exposed to 0.01% DMSO, the same percentage as in the staurosporine-treated cells.

Based on cell viability experiments, 100 μg/ml ganciclovir (Cytovene-IV; Roche Laboratories, Nutley, NJ), which gave 69% viability of C6VIK cells after 7 days of exposure, was used for culture experiments. C6VIK cells were plated at 1×10^5 per well in a 24-well plate. Twenty-four hours after plating, ganciclovir (100 μg/ml) was applied for time points ranging from 1 to 7 days. Fresh ganciclovir was added to media every other day. At each time point, media and drug were removed, cells washed twice with PBS, ICE-NIRF probe, and annexin were applied, and then TUNEL staining was carried out and the slides were evaluated 24 hours later by confocal microscopy.

Cell Viability Assays

Viability was assessed with the cell proliferation reagent, WST-1 (Roche Molecular Biochemicals, Penzberg, Germany), for Gli36 cells treated with the caspase-3 inhibitor and for C6VIK cells treated with ganciclovir. One thousand cells per well were plated in a 96-well plastic plate and, 24 hours later, the drug was added at the following concentrations: 5, 10, and 25 μM for DEVD-fmk and 50, 100, and 150 μg/ml for ganciclovir. Cells were exposed to the drug for 24 hours or 7 days, respectively, at which time media was aspirated and cells were incubated in 100 μl of fresh media and 10 μl of WST-1 reagent for 4 hours at 37°C in a 5% CO_2 incubator. Readings were taken on a Spectra max Plus 384 spectrophotometer (Molecular Devices Corporation) at 420 nm wavelength, and data were analyzed using Prism 3.03. Drug concentrations were tested in triplicate.

Granule Cell Preparation

Cultures enriched in granule neurons were prepared from dissociated cerebella of 5-day–old mice (129Sv/C57B6 mixed background), as described [42]. One day after culturing, the antimitotic drug, cytosine-D-arabinofuranoside (10 μM), was added to prevent proliferation of non-neuronal cells. After 3 days in culture, cells were irradiated with 14 Gy delivered from a ^{137}Cs source at 5.37 Gy/min. Twenty-four hours after irradiation, cells were incubated with the NIRF probe and annexin, as described above.

In Vivo NIRF Imaging

In an experimental *in vivo* implant model, Gli36 cells were infected in culture with HGCX-ICE-lacZ or HGCX vector at an MOI = 1.0. Four hours postinfection, cells were trypsinized, collected by centrifugation at 3000 × *g* for 5 minutes, and washed twice in PBS; and the 4×10^6 cells resuspended in 50 μl of PBS, mixed with 50 μl growth media, and then injected subcutaneously bilaterally under the forearms of five nude mice. Anesthesized mice were imaged 24 hours following intravenous (i.v.) probe administration of the ICE-NIRF probe (2 nmol of ICE-NIRF probe per animal) using a whole-body NIRF imaging system (CMIR, Charlestown, MA).

The imaging system consisted of a light-tight box equipped with a 150-W halogen lamp and an excitation filter system for Cy5.5 (610–650 nm; Omega Optical, Brattlerburo, VT). The field of view was homogenous to ± 10% over a 5 × 5-cm area through the use of fiberoptic cables and beam diffusers. Fluorescence was detected by a 12-bit monochrome CCD camera (Photometrics, Tuscon, AZ; Kodak, Rochester, NY) equipped with a C-mount lens and an emission filter at 700 nm (Omega Optical). Images were digitally acquired as 16-bit Tiff files and processed on a Macintosh computer using commercially available software (IP Lab Spectrum; Signal Analytics, Vienna, VA) [29]. Brightfield and NIRF images were collected and images superimposed. Quantification of fluorescence was done using CMIR image program by finding the mean pixel intensity of each implant infected with HGC-ICE or HGCX, as well as the background fluorescence from an adjacent region in each mouse.

Statistical Analysis

Statistical analysis was conducted using Microsoft Excel 97 SR-2. For cell culture experiments, a two-sample *t*-test assuming equal variances was conducted by comparing the average intensity of the probe signal across the microscopic field at 633 nm normalized to the average intensity of the EGFP signal at 488 nm between groups. For *in vivo* experiments, statistical analysis comparing the mean pixel intensities between treatment groups was conducted using a *t*-test: paired two sample for means, which gave a $P(T < -t)$ one-tail value.

Results

Specificity of NIRF Probe for Caspase-1

The specificity of the ICE-NIRF probe for caspase-1 (Figure 1*A*) was evaluated in two ways: 1) incubation of the probe with purified caspase-1 or caspase-3 *in vitro*; and 2)

incubation of HGC-ICE-lacZ vector–infected cells in culture with the probe in the presence of a caspase-1 inhibitor or a caspase-3 inhibitor. For *in vitro* testing, the probe was incubated with or without purified caspase-1 or caspase-3 over 30 minutes at room temperature. Incubation of the probe with purified caspase-1 resulted in a 78-fold increase in fluorescence (Figure 1*B*). Activation of the probe by caspase-1 was blocked over 95% by coincubation with a caspase-1–specific inhibitor. In comparison, the incubation of the probe with purified caspase-3 caused no changes in fluorescence signal.

In order to deliver the caspase-1–lacZ fusion protein to cells, coding sequences were placed under the CMV promoter in an amplicon plasmid, pHGCX [35], yielding pHGC-ICE-lacZ (Figure 2*A*). For convenient monitoring of gene expression, this construct includes a reporter EGFP cassette under an immediate early viral promoter (IE4/5). A parallel amplicon construct containing luciferase under the CMV promoter, pHGC-Fluc, was used as a control vector.

Gli36 cells were infected with packaged HGC-ICE-lacZ or control vector at an MOI = 1. Twenty-four hours following infection, cells evaluated for ICE-NIRF probe fluorescence indicated a specific signal in HGC-ICE-lacZ vector–infected cells (Figure 2*D*). Infection of Gli36 cells with the HGC-ICE-lacZ vector also induced apoptosis indicated by positive TUNEL staining (Figure 2*C*) concomitant with activation of the ICE-NIRF probe. Both apoptosis and probe activation were substantially blocked by incubation of cells infected with the HGC-ICE-lacZ vector with the caspase-1 inhibitor, YVAD-cmk, indicating specificity for caspase-1 (Figure 2, *F* and *G*). Infection of Gli36 cells with the control vector, HGC-Fluc, did not induce apoptosis, indicated by the

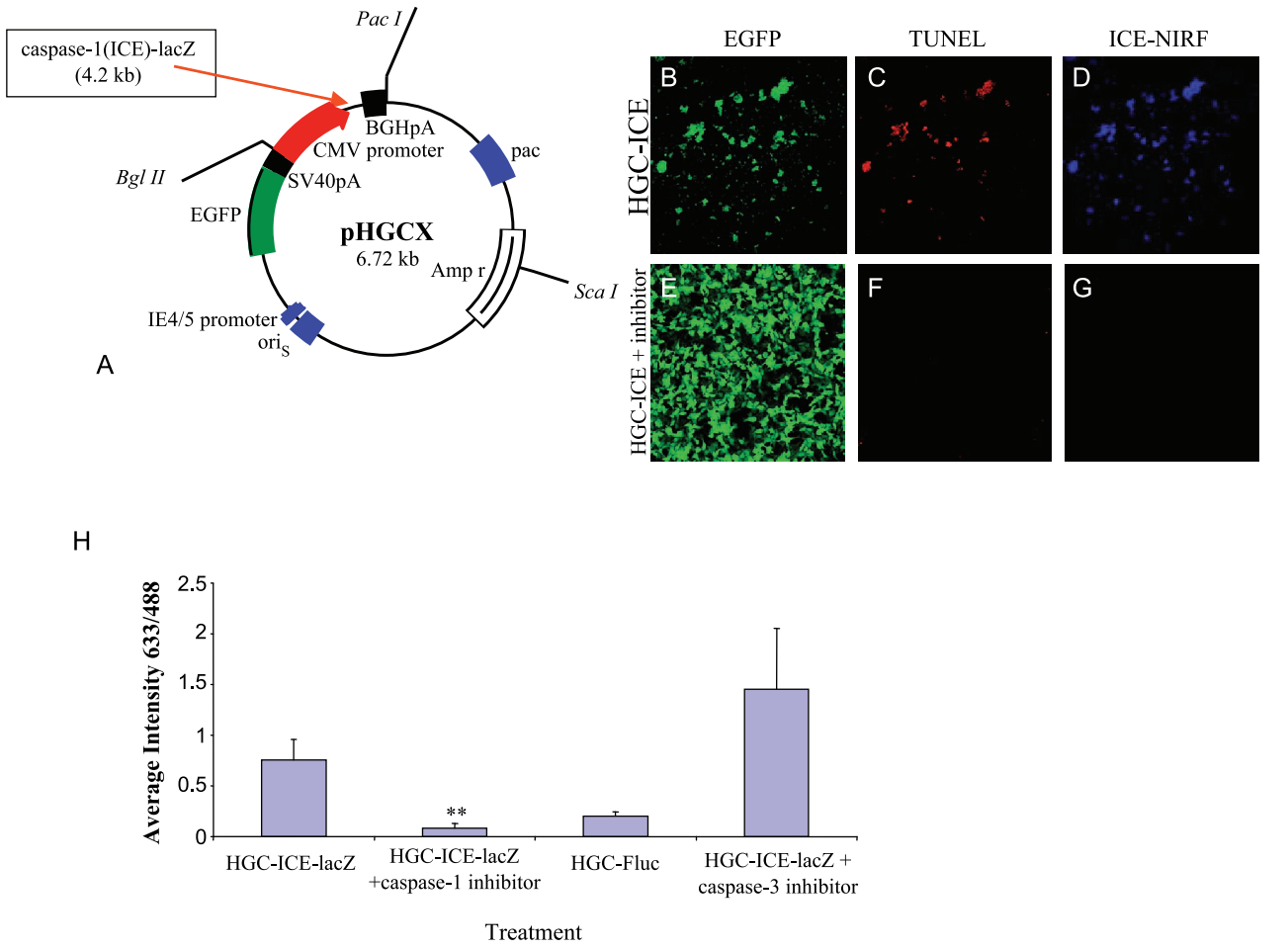

Figure 2. *HSV amplicon vector expressing caspase-1–lacZ induces apoptosis and activates ICE-NIRF probe. (A) pHGC-ICE-lacZ amplicon. ICE–lacZ cDNA was cloned into the multicloning site of the HSV amplicon pHGCX under the control of a CMV promoter. The pHGCX backbone contains an HSV origin of replication (ori_s), a cleavage/packaging signal (pac), as well as EGFP, under an intermediate early viral promoter, IE4/5 [36]. Infection of Gli36 with the HGC-ICE-lacZ vector (B and E; EGFP fluorescence) induces apoptosis, indicated by positive TUNEL staining (C) and activation of the caspase-1 NIRF probe (D). Vector-induced apoptosis is blocked by coincubation of the infected cells with the caspase-1 inhibitor, YVAD-cmk, indicated by a reduced number of TUNEL-stained cells (F) and lower-level activation of the ICE-NIRF probe (G). (Panels B–G used × 10 magnification.) (H) Quantification of the effect of caspase-1 and caspase-3 inhibitors on HGC-ICE-lacZ vector–induced activation of the ICE–NIRF probe. Gli36 cells were infected with caspase-1 or control (HGC-Fluc) vectors in the presence or absence of caspase inhibitors and fluorescence was assessed 24 hours later. Probe signal intensity was normalized to infection efficiency (EGFP signal). The caspase-1 inhibitor, YVAD-cmk, prevented HGC-ICE-lacZ vector–induced activation of the probe (a two-sample t-test assuming equal variances indicated a significant difference, P one-tail = .0157, n = 3). The caspase-3 inhibitor, DEVD-fmk, did not significantly affect HGC-ICE-lacZ–induced activation of the probe ($P \leq .166$).*

absence of TUNEL staining, nor did it produce a NIRF fluorescence signal (data not shown).

The effect of caspase-1 and caspase-3 inhibitors on HGC-ICE-lacZ–induced activation of the ICE-NIRF probe by Gli36 cells was quantified by determining the average intensity of the probe signal across the microscopic field at 633 nm and normalizing that to the average intensity of the EGFP signal at 488 nm (Figure 2*H*). The caspase-1 inhibitor prevented HGC-ICE-lacZ vector–mediated activation of the probe. A two-sample *t*-test assuming equal variances indicated that this difference was significant (P one-tail $\leq .0157$, $n = 3$). However, there was no significant difference in NIRF probe activation by HGC-ICE-lacZ in the absence or presence of the caspase-3 inhibitor ($P \leq .166$), and the control vector did not activate the probe.

ICE-NIRF Probe Detects Apoptosis in Cultured Cells

Several standard methods for inducing apoptosis were used to determine whether this ICE-NIRF probe could be used to monitor caspase-1 activity during externally elicited apoptosis in living cells in culture. One such method for inducing apoptosis involves treating cells with staurosporine [43], a microbial alkaloid, which inhibits protein kinases [44]. Treatment of Gli36 glioma cells with 50 μM staurosporine for 24 hours induced apoptosis, as assessed by positive annexin staining (Figure 3*A*), and also activated the ICE-NIRF probe (Figure 3*B*). Control cells treated with 0.01% DMSO, the same percentage as in the experimental treatment, did not show significant annexin staining (Figure 3*D*) or an ICE-NIRF signal (Figure 3*E*). In order to examine the specific role of caspase-1 in staurosporine-induced

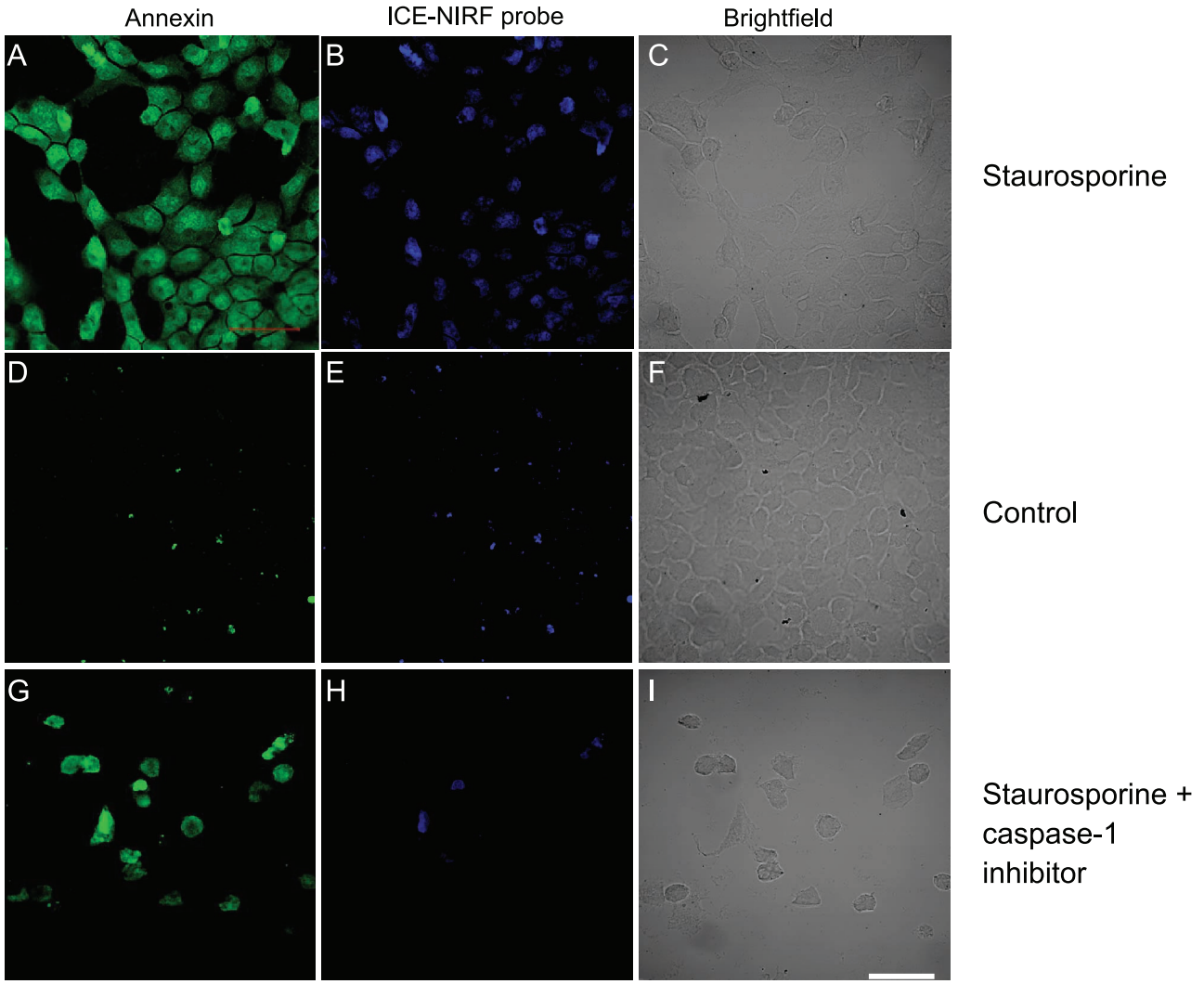

Figure 3. *Induction of apoptosis with staurosporine resulting in activation of the ICE-NIRF probe. Gli36 cells were treated with 50 μM staurosporine for 24 hours (A–C) or with the same percentage of DMSO (0.01%) to which experimental wells were exposed (D-488nm laser, E-633nm laser and F-bright field). To examine the role of caspase-1 in staurosporine-induced apoptosis and probe activation, cells were coincubated in caspase-1 inhibitor (10 μM) and staurosporine (G–I). Staurosporine induces apoptosis, indicated by the positive annexin staining viewed with the 488-nm laser (A), which colocalized with activated probe viewed with the 633-nm laser (B). Coincubation of the caspase-1 inhibitor with staurosporine did not completely block apoptosis, indicated by the relatively higher number of apoptotic cells stained with annexin (G), as those that activated the probe (H). Magnification, × 40; scale bar, 50 μM.*

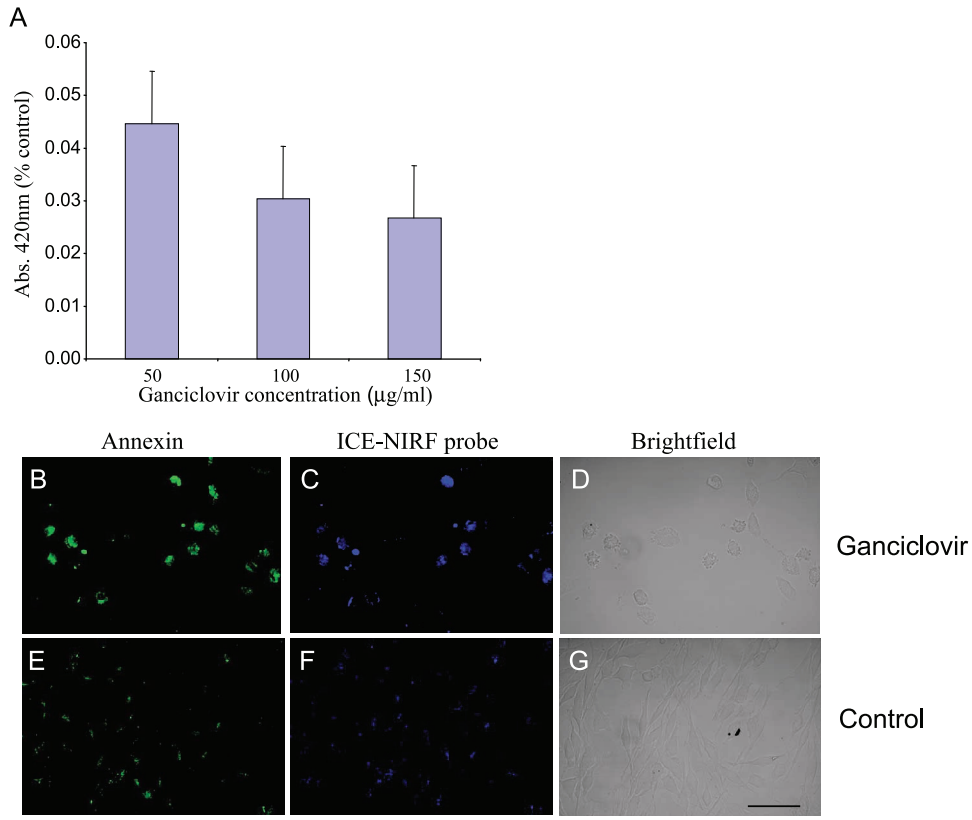

Figure 4. *Treatment of C6BVIK cells expressing HSV-TK with ganciclovir induces apoptosis and activates caspase-1 NIRF probe. (A) C6BVIK cells were treated with 50 to 150 μg/ml ganciclovir and assayed for cell viability using a WST assay. Concentrations of 50, 100, and 150 μg/ml ganciclovir resulted in significant cell death as compared to control treatments ($P \leq .001$). (B–G) C6BVIK cells were treated with 100 μg/ml ganciclovir for 3 days, prior to being treated with ICE-NIRF probe and annexin. Treatment with ganciclovir induced apoptosis, assessed by positive annexin staining (B), and activated the ICE-NIRF probe (C). Control C6BVIK cells not treated with ganciclovir did not stain for annexin (E) or demonstrate ICE-NIRF fluorescence (F). Magnification, × 40; scale bar, 50 μM.*

apoptosis and probe activation, cells were coincubated with both the caspase-1 inhibitor and staurosporine prior to treatment with probe and annexin (Figure 3*G–I*). The caspase-1 inhibitor decreased probe activation (Figure 3*H*), but did not completely block apoptosis (Figure 3*G*). Thus, a single caspase inhibitor for caspase-1 was not enough to save the cells from apoptosis triggered by staurosporine, but did block activation of the ICE-NIRF probe. Quantification of fluorescence intensity indicated that, overall, the caspase-1 inhibitor reduced staurosporine-induced ICE-NIRF activation by 80%.

Prior studies have demonstrated that C6BVIK glioma cells stably expressing HSV-TK die in response to treatment with ganciclovir [38] and that ganciclovir kills by apoptosis [45]. Viral TK is a prodrug-activating enzyme, which converts ganciclovir to a toxic nucleoside analogue. First, C6BVIK cells were treated with concentrations of ganciclovir ranging from 50 to 150 μg/ml for 7 days and assayed for cell viability using a WST assay. All concentrations resulted in significant cell death as compared to their respective controls ($P \leq .01$) with about 40% loss of viability at 150 μg/ml ganciclovir (Figure 4*A*). C6BVIK cells treated with ganciclovir for 1 to 7 days were also assessed for apoptosis and probe activation by staining with annexin and the ICE-NIRF probe. For time points 3 to 7 days in the presence of ganciclovir (100 μg/ml), condensed apoptotic nuclei were visible with 4′-6-diamidino-2-phenylindole dihydrochloride (DAPI) or PI staining (data not shown). C6BVIK cells treated with ganciclovir at 100 μg/ml for 3 days yielded positive annexin staining (Figure 4*B*) and ICE-NIRF probe activation (Figure 4*C*). Untreated C6BVIK cells did not stain positively for annexin (Figure 4*E*) or demonstrate ICE-NIRF fluorescence (Figure 4*F*).

We also examined whether induction of apoptosis by irradiation of primary neuronal cultures of cerebellar granule cells would lead to activation of the ICE-NIRF probe. Previous studies have shown that irradiation of the cerebellum of newborn mice results in extensive apoptosis in the external granule layer [46]. Cultured granule cells from newborn mice were irradiated and, 24 hours later, cultures were incubated with ICE-NIRF probe and stained with annexin. Positive annexin staining was observed in irradiated granular cells (Figure 5*A*) in parallel with activation of the ICE-NIRF probe (Figure 5*B*). Minimal cellular annexin staining and no detectable ICE-NIRF activation were observed in nonirradiated granule cells (Figure 5, *D* and *E*, respectively).

In Vivo Imaging

In an experimental *in vivo* tumor implant model, Gli36 cells were infected in culture with HGC-ICE-lacZ or HGCX

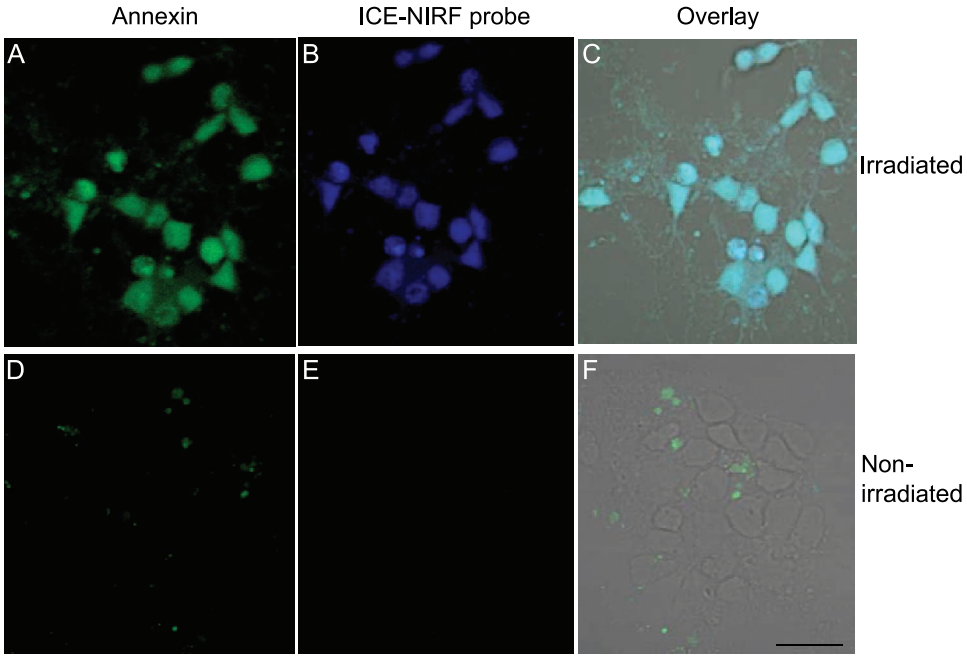

Figure 5. *Induction of apoptosis by irradiation of cerebellar granule cells activates ICE-NIRF probe. Twenty-four hours following irradiation, cultured cells were incubated with probe and stained with annexin. Positive annexin staining (A) and activation of the ICE-NIRF probe (B) were observed in irradiated granule cells. No annexin staining or ICE-NIRF probe activation was noted in nonirradiated cultures. Overlays of the fields were observed with the annexin, ICE-NIRF signals, and brightfield image (C and F). Magnification, × 40; scale bar, 50 μM.*

virus vectors at an MOI = 1 for 4 hours, which yielded > 95% infection of cells. Infected cells were implanted bilaterally (4×10^6 per site) in the forearms of five nude mice. Twenty-four hours later, the ICE-NIRF probe was injected i.v. and the mice imaged 24 hours after probe administration. The mean pixel intensity of the HGC-ICE-lacZ–infected Gli36 implant was 769.3 AU (SD + 209.2), whereas that of the HGCX-infected implant was 630.6 AU (SD + 101.0), and the background in an adjacent area was 436.3 (SD + 77.7). This background area had low endogenous fluorescence, whereas nonspecific probe fluorescence was somewhat higher in the liver, spleen, and bladder, as seen for other NIRF probes [28]. Subtracting the adjacent background from the implant values, there was significantly ($P \leq .006$) more fluorescence in HGC-ICE-lacZ–infected cells by 76% than in HGCX-infected cells. A pseudocolor image of the mean pixel intensities of NIRF fluorescence minus the background in implants in one of these mice indicates that this increase in intensity is visually notable (Figure 6). Of note, the NIRF fluorescence of the HGCX-infected cell implant was significantly ($P \leq .048$) higher than the adjacent normal tissue, suggesting that the vector or injectate volume may have triggered tissue damage and apoptosis. A direct comparison of the fluorescence between the HGC-ICE-lacZ–infected cell implant and adjacent normal tissues indicated a 1.7-fold increase in mean intensity.

Discussion

Here, we describe the development and characterization of a caspase-1 (ICE)–specific NIRF probe as a means to non-invasively image apoptosis in living cells. Specificity was shown by selective probe activation with caspase-1, and not caspase-3, and inhibition of activation by a caspase-1 inhibitor, and not a caspase-3 inhibitor. Furthermore, induction of apoptosis and probe activation was demonstrated following delivery of a caspase-1–lacZ fusion protein to cells in culture using an HSV amplicon vector. Three different methods of inducing apoptosis—staurosporine treatment, exposure of cells expressing HSV-TK to ganciclovir, and irradiation of cerebellar granule cells—all led to activation of this ICE-NIRF probe. The caspase-1 inhibitor partially blocked staurosporine-induced activation of the probe, but did not completely block apoptosis, suggesting that staurosporine induces apoptosis by activating multiple caspase pathways, some independent of caspase-1, such as activation of the CED-3 family of proteases [47].

Caspase-1 has been implicated in apoptosis of a number of cell types. Caspase-1 activity is present in cells throughout the lifespan of mice and may be an early mediator of cell death during some types of neuronal degeneration, with caspase-1 acting as a chronic initiator and caspase-3 acting as the final executioner of cell death. Caspase-1–deficient mice show delayed neutrophil apoptosis and a prolonged inflammatory response to lipopolysaccharide-induced acute lung injury, but otherwise normal development and physiology [48]. Caspase-1 is activated as an early event in the death of motor neurons in transgenic mouse lines expressing a mutant form of Cu^{2+},Zn^{2+} superoxide dismutase, which develop familial amyotrophic lateral sclerosis–like disease [20]. In these animals, activation of caspase-1 is followed by activation of

caspase-3 and the appearance of apoptotic neurons and astrocytes specifically in affected regions.

Our laboratory has previously expressed the ICE–lacZ fusion protein in experimental cancer therapy using a tetracycline-regulated retrovirus vector [49]. In the case of slow-growing, benign tumors, where reduction in volume can be therapeutic and the rate of DNA replication may not make cells susceptible to DNA-damaging agents, delivery of apoptotic proteins, such as ICE–lacZ, may prove efficacious. Targeting could be achieved by direct injection of vectors into the tumor mass with consequent volume reduction. In this context, NIRF imaging could allow direct monitoring of therapeutic gene expression.

Currently, most ways of studying apoptosis rely on experiments done on cell extracts in the test tube or imaging of cells in culture or tissue sections. The former includes DNA fragmentation or fluorogenic assays using fluorescently labeled substrates for various caspases, and the latter includes surface labeling of annexin V, nuclear staining with PI or TUNEL, or assessment of caspase activities in intact cells using cell-permeable fluorogenic caspase substrates. Recently, a fluorescent Cy5.5–annexin V–NIRF probe has shown promise in imaging apoptosis in living animals [50]. The key issue in converting annexin V from a cellular imaging agent to an *in vivo* imaging agent was the use of a fluorochrome, which emits fluorescence light in the near-infrared range. Light in the NIRF range allows much deeper tissue penetration, as well as less nonspecific tissue autofluorescence and reflectance [51].

The potential for imaging of caspase-1 activity *in vivo* with the ICE-NIRF probe was evaluated in an experimental tumor implantation model. Glioma cells were infected in culture with an HSV amplicon vector encoding caspase-1–lacZ (HGC-ICE-lacZ) or a control vector, implanted in mice, and evaluated 48 hours later after i.v. ICE-NIRF probe injection. There was a significant increase (76%) in fluorescence in the ICE–lacZ vector–infected cells, with a greater increase (171%) between ICE–lacZ vector–infected cells and adjacent normal tissue background. The low—but greater than background—levels of ICE-NIRF fluorescence observed in the implants infected with control amplicon vector may be due to apoptosis induced by the vector or injectate. These *in vivo* data suggest that this ICE-NIRF probe has the potential to image caspase-1 activity and apoptosis, depending on enzyme levels and tissue depth.

Compared to other methods, imaging apoptosis with an ICE-NIRF probe has the potential advantage of allowing much deeper tissue penetration, with less nonspecific tissue autofluorescence, as compared to imaging using a recombinant luciferase reporter molecule and bioluminescence imaging, as photons do not allow deep tissue penetration [27]. Furthermore, given the numerous types of caspases with roles in different biologic processes, it will be highly advantageous to have probes for *in vivo* imaging that are specific to the different caspases. Over the past few years, we have applied several NIRF protease activatable probes to various biological systems and have shown great promise of imaging disease processes through their associated protease activity [35,52]. The applications include cancer,

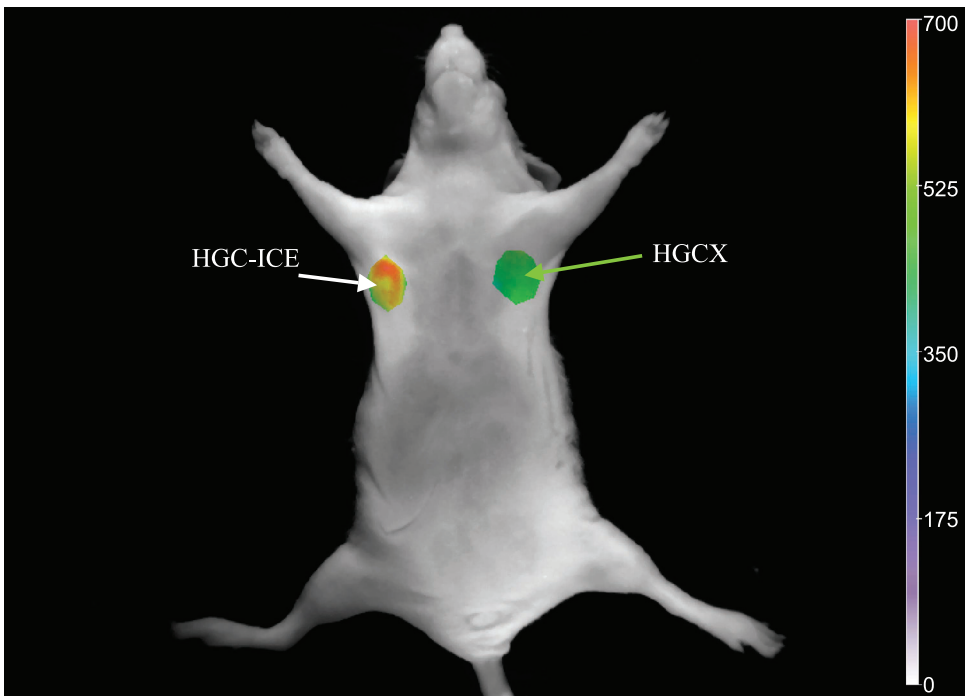

Figure 6. *Pseudocolor image of caspase-1 activity in vivo. HGC-ICE-lacZ–infected Gli36 cells were implanted into the left side of a nude mouse and HGCX-infected Gli36 cells into the right side. Animals were imaged 48 hours after injection of cells, 24 hours after tail vein injection of ICE-NIRF probe. The mean pixel intensity in HGC-ICE-lacZ–infected cells (indicated by white arrow) for this particular animal was 843 AU, as compared to 755 AU for the HGCX-infected cells (green arrow) and 347 AU for adjacent normal tissue (background). Pseudocolor images represent implant intensities minus the background.*

arteriosclerosis, arthritis, blood coagulation, inflammation, and others. In conclusion, this novel ICE-NIRF imaging probe allows high-sensitivity imaging of apoptosis involving caspase-1 activation in living cells. It should have important applications in imaging results of therapeutic intervention in cancer, extent of cell damage in injury models, and normal apoptotic mechanisms in development.

Acknowledgements

We thank Suzanne McDavitt for skilled editorial assistance and Dr. Jungying Yuan (Harvard Medical School) for providing the plasmid pBSMIOZ containing the caspase-1–lacZ cassette.

References

[1] Nicholson DW (1996). ICE/CED3–like proteases as therapeutic targets for the control of inappropriate apoptosis. *Nat Biotechnol* **14,** 297–301.

[2] Reed JC (2002). Apoptosis-based therapies. *Nat Rev Drug Discov* **1,** 111–121.

[3] Thornberry N and Lazebnik Y (1998). Caspases: enemies within *Science* **281,** 1312–1316.

[4] Blanco FJ, Ochs RL, Schwarz H, and Lotz M (1995). Chondrocyte apoptosis induced by nitric oxide. *Am J Pathol* **146,** 75–85.

[5] Bustamante J, Bersier G, Romero M, Badin RA, and Boveris A (2000). Nitric oxide production and mitochondrial dysfunction during rat thymocyte apoptosis. *Arch Biochem Biophys* **376,** 239–247.

[6] Kim YM, Chung HT, Simmons RL, and Billiar TR (2000). Cellular nonheme iron content is a determinant of nitric oxide–mediated apoptosis, necrosis, and caspase inhibition. *J Biol Chem* **275,** 10954–10961.

[7] Salvesen GS and Dixit VM (1997). Caspases: intracellular signaling by proteolysis. *Cell* **91,** 443–446.

[8] Nicholson DW and Thornberry NA (1997). Caspases: killer proteases. *Trends Biochem Sci* **22,** 299–306.

[9] Grutter MG (2000). Caspases: key players in programmed cell death. *Curr Opin Struct Biol* **10,** 649–655.

[10] Nicholson DW (1999). Caspase structure, proteolytic substrates, and function during apoptotic cell death. *Cell Death Differ* **6,** 1028–1042.

[11] Thornberry NA, Bull HG, Calaycay JR, Chapman KT, Howard AD, Kostura MJ, Miller DK, Molineaux SM, Weidner JR, and Aunins J (1992). A novel heterodimeric cysteine protease is required for interleukin-1 β processing in monocytes. *Nature* **356,** 768–774.

[12] Wang S, Miura M, Jung Y, Zhu H, Li E, and Yuan J (1998). Murine caspase-11, an ICE-interacting protease, is essential for the activation of ICE. *Cell* **92,** 501–509.

[13] Kang SJ, Wang S, Hara H, Peterson EP, Namura S, Hanjani AS, Huang Z, Srinivasan A, Tomaselli KJ, Thornberry NA, Moskowitz MA, and Yuan J (2000). Dual role of caspase-11 in mediating activation of caspase-1 and caspase-3 under pathological conditions. *J Cell Biol* **149,** 613–622.

[14] Shibata M, Hisahara S, Hara H, Yamawaki T, Fukuuchi Y, Yuan J, Ohano H, and Miura M (2000). Caspases determine the vulnerability of oligodendrocytes in the ischemic brain. *J Clin Invest* **106,** 643–653.

[15] Miura M, Zhu H, Rotello R, Hartwieg EA, and Yuan J (1993). Induction of apoptosis in fibroblasts by IL-1-β–converting enzyme, a mammalian homolog of the *C. elegans*. *Cell* **75,** 653–660.

[16] Alnemri ES, Livingston DJ, Nicholson DW, Salvesen G, Thornberry NA, Wongsd WW, and Juan J (1996). Human ICE/CED-3 protease nomenclature. *Cell* **87,** 171.

[17] White M (1996). ICE/CED-3 proteases in apoptosis. *Trends Cell Biol* **6,** 245–248.

[18] Guo Y and Kyprianou N (1999). Restoration of transforming growth factor beta signaling in human prostate cancer cells suppresses tumorigenicity via induction of caspase-1 mediated apoptosis. *Cancer Res* **59,** 1366–1371.

[19] Winter RN, Cramer A, Borkowski A, and Krprianou N (2001). Loss of caspase-1 and caspase-3 protein expression in human prostate cancer. *Cancer Res* **61,** 1227–1232.

[20] Pasinelli P, Houseweart MK, Brown RH, and Cleveland DW (2000). Caspase-1 and caspase-3 are sequentially activated in motor neuron death in Cu,Zn superoxide dismutase–mediated familial amyotrophic lateral sclerosis. *Proc Natl Acad Sci USA* **97,** 13901–13906.

[21] Wood BL, Gibson DF, and Tait JF (1996). Increased erythrocyte phosphatidylserine exposure in sickle cell disease: flow-cytometric measurement and clinical associations. *Blood* **88,** 1873–1880.

[22] Rao JK, Letada P, Haverstick DM, Herman MM, and Savory J (1998). Modifications to the *in situ* TUNEL method for detection of apoptosis in paraffin-embedded tissue sections. *Ann Clin Lab Sci* **28,** 131–137.

[23] Whiteside G, Cougnon N, Hunt SP, and Munglani R (1998). An improved method for detection of apoptosis in tissue sections and cell culture, using the TUNEL technique combined with Hoechst stain. *Brain Res Brain Res Protoc* **2,** 160–164.

[24] Whiteside G and Munglani R (1998). TUNEL, Hoechst and immunohistochemistry triple-labeling: an improved method for detection of apoptosis in tissue sections—an update. *Brain Res Brain Res Protoc* **3,** 42–53.

[25] Charriaut-Marlangue C and Ben-Ari Y (1995). A cautionary note on the use of the TUNEL stain to determine apoptosis. *Neuroreport* **7,** 61–64.

[26] Yasuda M, Umermura S, Osamura RY, Kenjo T, and Tsutsumi Y (1995). Apoptotic cells in the human endometrium and placental villi: pitfalls in applying the TUNEL method. *Arch Histol Cytol* **58,** 185–190.

[27] Laxman B, Hall DE, Bhoani MS, Hamstra DA, Chenevert TL, Ross BD, and Rehemtulla A (2002). Noninvasive real-time imaging of apoptosis. *Proc Natl Acad Sci USA* **99,** 16551–16555.

[28] Tung CH, Bredow S, Mahmood U, and Weissleder R (1999). Preparation of a cathepsin D sensitive near-infrared fluorescence probe for imaging. *Bioconjug Chem* **10,** 892–896.

[29] Weissleder R, Tung CH, Mahmood U, and Bogdanov A Jr (1999). *In vivo* imaging of tumors with protease-activated near infrared fluorescent probes. *Nat Biotechnol* **17,** 375–778.

[30] Bremer C, Bredow S, Mahmood U, Weissleder R, and Tung CH (2001). Optical imaging of Matrix Metalloprotease-2 (MMP-2) enzyme activity: a marker for angiogenesis and tumor progression. *Radiology* **221,** 523–529.

[31] Bremer C, Tung CH, and Weissleder R (2001). *In vivo* molecular target assessment of matrix metalloproteinase inhibition. *Nat Med* **7,** 743–748.

[32] Jaffer FA, Tung CH, Gerszten RE, and Weissleder R (2002). *In vivo* imaging of thrombin activity in experimental thrombi using a thrombin-sensitive near-infrared molecular probe. *Arterioscler Thromb Vasc Biol* **22,** 1929–1935.

[33] Tung CH, Gerszten RE, Jaffer FA, and Weissleder R (2002). A novel near infrared fluorescence sensor for detection of thrombin activation in blood. *Chembiolchem* **3,** 207–211.

[34] Shah K, Tang Y, Breakefield XO, and Weissleder R (2003). Real time imaging of TRAIL induced apoptosis of glioma tumors *in vivo*. *Oncogene* **22**, 6865–6872.

[35] Funovics M, Weissleder R, and Tung CH (2003). Protease sensors for bioimaging. *Anal Bioanal Chem* **377,** 956–9633.

[36] Saeki Y, Fraefel C, Ichikawa T, Breakefield XO, and Chiocca EA (2001). Improved helper virus–free packaging system for HSV amplicon vectors using an ICP27-deleted, oversized HSV-1 DNA in a Bacterial Artificial Chromosome. *Mol Ther* **3,** 591–601.

[37] Benda P, Lightbody J, Sato G, Levine L, and Sweet W (1968). Differentiated rat glial cell strain in tissue culture. *Science* **161,** 370–371.

[38] Ezzeddine ZD, Martuza RL, Platika D, Short MP, Malick A, Choi B, and Breakefield XO (1991). Selective killing by glioma cells in culture and *in vivo* by retrovirus transfer of the herpes simplex virus thymidine kinase gene. *New Biol* **3,** 608–614.

[39] Smith IL, Hardwicke MA, and Sandri-Goldin RM (1992). Evidence that the herpes simplex virus immediate protein ICP27 acts post-transcriptionally during infection to regulate gene expression. *Virology* **186,** 74–86.

[40] Pennington MW and Thornberry NA (1994). Synthesis of a fluorogenic interleukin-1 beta converting enzyme substrate based on resonance energy transfer. *Pept Res* **7,** 72–76.

[41] Spreafico R, Arcelli P, Frassoni C, Canetti P, Gliaccone G, Rizzuti T, Mastrangelo M, and Bentivoglio M (1999). Development of layer I of the human cerebral cortex after midgestation: architectonic findings, immunocytochemical identification of neurons and glia, and *in situ* labeling of apoptotic cells. *J Comp Neurol* **410,** 126–142.

[42] Hatten ME, Gao W-Q, Morrison ME, and Mason CA (1998). The cerebellum: purification and co-culture of identified cell populations. In Banker, G, Goslin, K (Eds.), Culturing Nerve Cells, pp. 419–459 MIT Press, Cambridge, MA.

[43] Zhu H, Fearnhead HO, and Cohen GM (1995). An ICE-like protease is a common mediator of apoptosis induced by diverse stimuli in human monocytic THP.1 cells. *FEBS Lett* **374,** 303–308.

[44] Chae H-J, Kang J-S, Byun J-O, Han K-S, Kim D-U, Oh S-M, Kim H-M, Chae S-W, and Kim H-R (2000). Molecular mechanisms of staurosporine-induced apoptosis in osteoblasts. *Pharmacol Res* **42,** 373–381.

[45] Shaw MM, Gurr WK, Watts PA, Littler E, and Field HJ (2001). Ganciclovir and penciclovir, but no acyclovir, induce apoptosis in herpes simplex virus thymidine kinase–transformed baby hamster kidney cells. *Antivir Chem Chemother* **12,** 175–186.

[46] Herzog KH, Chong MJ, Kapsetaki M, Morgan JI, and McKinnon PJ (1998). Requirement for Atm in ionizing radiation–induced cell death in the developing central nervous system. *Science* **280,** 1089–1091.

[47] Srinivasan A, Foster LM, Testa MP, Ord T, Keane RW, Bredesen DE, and Kayalar C (1996). Bcl-2 expression in neural cells blocks activation of ICE/CED-3 family proteases during development. *J Neurosci* **16,** 5654–5660.

[48] Rowe SJ, Allen L, Ridger VC, Hellewell PG, and Whyte MKB (2002). Caspase-1–deficient mice have delayed neutrophil apoptosis and a prolonged inflammatory response to lipopolysaccharide-induced acute lung injury. *J Immunol* **69,** 6401–6407.

[49] Yu JS, Sena-Esteves M, Paulus W, Breakefield XO, and Reeves SA (1996). Retroviral delivery and tetracycline-dependent expression of 1L-1β-converting enzyme (ICE) in a rat glioma model provides controlled induction of apoptotic death in tumor cells. *Cancer Res* **56,** 5423–5427.

[50] Petrovsky A, Schellenberger E, Josephson L, Weissleder R, and Bogdanov A Jr (2003). Near-infrared fluorescent imaging of tumor apoptosis. *Cancer Res* **63,** 1936–1942.

[51] Ntziachristos V, Ripoll J, and Weissleder R (2002). Can near-infrared fluorescence propagate through human organs for non-invasive clinical examinations? *Opt Lett* **27,** 333–335.

[52] Shah K, Tung C, Chang C, Slootweg E, O'Loughlin T, Breakefield XO, and Weissleder R (2004). *In vivo* imaging of HIV protease activity in amplicon vector transduced gliomas. *Cancer Res* **64**, 273–278.